Biochimica et Biophysica Acta 1828 (2013) 2757–2762

Contents lists available at ScienceDirect

Biochimica et Biophysica Acta

journal homepage: www.elsevier.com/locate/bbamem

The sticholysin family of pore-forming toxins induces the mixing of lipids in membrane domains

Uris Ros [a], Michelle A. Edwards [b], Raquel F. Epand [c], Maria E. Lanio [a], Shirley Schreier [d], Christopher M. Yip [b], Carlos Alvarez [a], Richard M. Epand [c,*]

[a] Center for Protein Studies, Biology Faculty, University of Havana, Havana CP 10400, Cuba
[b] Institute of Biomaterials and Biomedical Engineering, Terrence Donnelly Centre for Cellular and Biomolecular Research, University of Toronto, Toronto M5S 3E1, Canada
[c] Department of Biochemistry and Biomedical Sciences, McMaster University Health Science Center, Hamilton, Ontario L8S 4K1, Canada
[d] Department of Biochemistry, Institute of Chemistry, University of São Paulo, C.P. 26077, 05513-970 São Paulo, SP, Brazil

ARTICLE INFO

Article history:
Received 6 May 2013
Received in revised form 30 July 2013
Accepted 2 August 2013
Available online 14 August 2013

Keywords:
Sticholysin
Actinoporin
Pore-forming toxin
Lipid phase separation
Lipid mixing
Toroidal pore

ABSTRACT

Sticholysins (Sts) I and II (StI/II) are pore-forming toxins (PFTs) produced by the Caribbean Sea anemone *Stichodactyla helianthus* belonging to the actinoporin family, a unique class of eukaryotic PFTs exclusively found in sea anemones. The role of lipid phase co-existence in the mechanism of the action of membranolytic proteins and peptides is not clearly understood. As for actinoporins, it has been proposed that phase separation promotes pore forming activity. However little is known about the effect of sticholysins on the phase separation of lipids in membranes. To gain insight into the mechanism of action of sticholysins, we evaluated the effect of these proteins on lipid segregation using differential scanning calorimetry (DSC) and atomic force microscopy (AFM). New evidence was obtained reflecting that these proteins reduce line tension in the membrane by promoting lipid mixing. In terms of the relevance for the mechanism of action of actinoporins, we hypothesize that expanding lipid disordered phases into lipid ordered phases decreases the lipid packing at the borders of the lipid raft, turning it into a more suitable environment for N-terminal insertion and pore formation.

1. Introduction

Pore-forming toxins (PFTs) are primitive but lethal agents that play an active role in the defense system of bacteria, plants, invertebrates, and vertebrates [1]. Sticholysins (StI and StII) are two potent cytolysins purified from the sea anemone *Stichodactyla helianthus* [2]. They are classified into the group of actinoporins, cytolytic polypeptides, exclusively found in sea anemones belonging to the protein super-family of PFTs [3,4]. Actinoporins are soluble, cysteine-less proteins, with molecular weight around 20 kDa and whose putative receptor is sphingomyelin (SM) [4,5]. To date, the structures of equinatoxin II (EqtII), an actinoporin purified from *Actinia equina* [6,7], StI [8], StII [9], and fragaceatoxin C (FraC) produced by *Actinia fragacea* [10] have been solved. These toxins contain a β-sandwich core, flanked on opposite sides by two α-helices. The mechanism of pore formation proposed for actinoporins is based on an initial binding step followed by oligomerization and membrane insertion leading to pore formation [11]. The first thirty N-terminal amino acid residues of these toxins, which includes an amphipathic α-helix, is the most probable sequence involved in membrane insertion [9–17].

The nature of the interaction between actinoporins and lipids in membranes and, in particular, the specific role of SM in pore formation are poorly understood. One remarkable characteristic of actinoporins is the fact that their affinity for membranes is greatly enhanced by the presence of SM [18–22] and/or by the coexistence of lipid phases in the target membrane [23–26]. Therefore, the role of SM, phase state of lipid bilayers, and packing defects related to the occurrence of lipid microdomains have all been claimed to modify the toxin's ability to bind to the membrane, insert and subsequently cause pore formation.

In the present study, we investigated the effect of sticholysins on lipid membrane organization. In spite of the high sequence homology existing between both sticholysins (93%), we included both StI and II in this study since the two proteins show different activities, which may be reflected in their membrane binding properties [26]. We analyzed the effect of the proteins on lipid phase separation on membranes using Differential Scanning Calorimetry (DSC) and Atomic Force Microscopy (AFM). These results provided further insight into the molecular mechanism of action of actinoporins. Namely, we propose that sticholysins promote the mixing of lipids from existing membrane domains, which could be relevant to their oligomerization state, their N-terminus insertion into the bilayer and subsequent pore formation.

Abbreviations: StI and StII, sticholysin I and II; PFTs, pore forming toxins; SM, Sphingomyelin; EqtII, equinatoxin II; FraC, fragaceatoxin C; DSC, Differential Scanning Calorimetry; AFM, Atomic Force Microscopy; DMPC, Dimyristoylphosphatidylcholine; DPPC, Dipalmitoylphosphatidylcholine; DOPC, Dioleoylphosphatidylcholine; eSM, egg sphingomyelin; Chol, cholesterol; MLV, multilamellar vesicles; SUV, small unilamellar vesicles; T_m, temperature of transition; ΔH, calorimetric enthalpies; Lo, liquid-ordered domain; Ld, liquid-disordered domain

* Corresponding author. Tel.: +1 905 525 9140x22073; fax: +1 905 521 1397.
E-mail address: epand@mcmaster.ca (R.M. Epand).

0005-2736/$ – see front matter © 2013 Elsevier B.V. All rights reserved.
http://dx.doi.org/10.1016/j.bbamem.2013.08.001

2. Materials and methods

2.1. Lipids

Dimyristoylphosphatidylcholine (DMPC), dipalmitoylphosphatidylcholine (DPPC), dioleoylphosphatidylcholine (DOPC), egg sphingomyelin (eSM), and cholesterol (Chol) were purchased from Avanti Polar Lipids (Alabaster, USA) and were used without further purification.

2.2. Sticholysin purification

StI and II were purified from *S. helianthus* and characterized according to Lanio et al. [2]. The fractions corresponding to each peak (StI and StII) were concentrated and diafiltrated with distilled water or the required buffer using an Amicon ultrafiltration device equipped with a membrane whose cut-off was 1000 Da. Protein concentration was determined employing absorption coefficients of 2.13 and 1.87 mL mg^{-1} cm^{-1} at 280 nm for StI and StII, respectively [2].

2.3. Sample preparations for measurements in DSC and AFM

For DSC studies, lipid films were made by dissolving appropriate amounts of lipids in chloroform/methanol 2:1 (v/v) followed by solvent evaporation under a stream of nitrogen to deposit the lipid as a film on the walls of a tube. The tube was placed in a vacuum chamber for at least 2 h to remove the last traces of solvent. Dried films were kept under argon gas at −20 °C until used. Films were hydrated with 20 mM PIPES buffer (1 mM EDTA, 150 mM NaCl, 0.002% NaN_3, and pH 7.4) in the presence or not of an appropriate amount of protein solution to obtain a specific lipid to protein ratio, and vortexed extensively to make multilamellar vesicles (MLV).

For the AFM studies, lipid stock solutions were mixed and dried in a test tube by rotoevaporation for a minimum of 1 h. HEPES buffer (10 mM HEPES, 150 mM NaCl, pH 7.4) was added, and the resulting lipid mixture was sonicated using an ultrasonic bath (VWR 50D Aquasonic) for 40 min at ~10 °C above than the highest transition temperature of any of the lipid components.

2.4. DSC measurements

Calorimetric scans were carried out on a MicroCal VP-DSC differential scanning calorimeter (Massachusetts, USA), using the software supplied by the manufacturer for data collection and analysis. The reference and the sample solutions were degassed at room temperature prior to scanning. The scan rate was 1 °C min^{-1} and there was a delay of 10 min between sequential scans in a series to allow thermal equilibration. The scans were recorded in the presence and in the absence of protein using PIPES buffer as the reference. The excess heat capacity of the samples was obtained by subtraction of the reference scan of buffer vs. buffer from the scan of the sample vs. buffer. The resulting scan was normalized by dividing by the number of moles of lipids in the sample cell. The temperature of transition (T_m) was measured as the maximum of excess heat capacity and the calorimetric enthalpy (ΔH) was calculated by integrating the peak areas. Gaussian two-peak fitting analysis with Origin 8.0 (OriginLab Corporation, USA) was performed to deconvolute the thermographs obtained from binary mixtures in the absence of the proteins.

2.5. In situ AFM measurements

A glass fluid cell for the Nanoscope IIIA MultiMode AFM (Bruker Nano Surfaces, Santa Barbara, CA, USA) was sealed on top of a freshly-cleaved piece of mica using an O-ring to create a 200 μL sample compartment. HEPES buffer (10 mM HEPES, 150 mM NaCl, pH 7.4) was injected in order to fill the fluid cell. In parallel, liposomes were diluted with HEPES to a volume of 500 μL and heated at 65 °C for 5 min. The heated liposomes were injected into the fluid cell and allowed to sit for 30 min, after which 1 mL of HEPES was injected to remove unfused liposomes. A 300 μL aliquot of HEPES buffer containing the protein of interest at the desired concentration was injected into the flow-through fluid cell. AFM images were acquired in fluid tapping mode with a Digital Instrument MultiMode equipped with a Nanoscope IIIA controller and operating under version 5.30R1 of the Nanoscope software (Bruker), a "J" scanner having a maximum lateral scan size of 116 μm by 116 μm (Bruker Nano Surfaces, Santa Barbara, CA, USA), and a SNL-10 short, thin tip (Veeco Probes, California, USA). Images were collected at a scan rate of 1 Hz, and scan angle of 0° as 512 × 512 pixel data sets. The drive frequency was usually set between 7 and 10 kHz with a drive amplitude set point of 0.2–0.6 V.

2.6. Reproducibility of measurements

The DSC and AFM measurements were repeated at least once, giving similar results. A representative set of data, run at the same time, is presented.

3. Results

3.1. Influence of sticholysins on the phase transition of eSM, DPPC, and DMPC pure lipids

Vesicles were composed of eSM, DPPC, or DMPC. eSM was selected as one of the lipid compositions since this phospholipid has been proposed as a putative receptor for actinoporins in the membrane [4]. Additionally, DPPC and DMPC were used to compare the effect of the proteins on the phase transition of other phospholipids having similar or lower melting temperatures, respectively. DSC curves obtained from heating cycles are presented as heat capacity per mole of lipids (Fig. 1) and the measured T_m and ΔH parameters are summarized in Table 1. Both pure eSM [27] and DPPC [28] are characterized by a sharp gel to liquid-crystalline main phase transition around 40 and 41 °C, respectively. However the eSM endotherm is broader compared with DPPC. Although the acyl chain composition of egg SM is highly enriched in C16:0 (84%) acyl chains, this natural lipid also contains other acyl chains as well [29]. As with DPPC, the pure synthetic DMPC undergoes a sharp gel to liquid-crystalline phase transition at 24 °C, as previously described [30]. The addition of sticholysins (lipid:protein ratio = 75) to the membrane did not result in significant transition temperature changes (within 0.1 °C) nor variation of the enthalpy of the transition (by more than 1 kcal/mol) (Fig. 1, Table 1). For eSM vesicles, even at higher sticholysin concentrations (lipid:protein ratio = 20), there was no effect on the phase transition properties (data not shown). There were also no significant changes on subsequent heating and cooling scans, indicating that the system was at equilibrium (data not shown).

3.2. Influence of sticholysins on the phase transition of binary mixtures of lipids

Binary mixtures (eSM:Chol, 9:1 and DPPC:Chol, 9:1) were selected taking into account that Chol can promote phase separation in phospholipid bilayers by altering the thermotropic phase behavior and organization of glycero- and sphingo-lipids. This low amount of Chol (10%) is enough for the detection of small domains in membranes without losing the main transition of the phospholipids [30]. Samples in the presence of Chol reached equilibrium after one heating and cooling cycle. Therefore, only scans subsequent to the first heating and cooling cycle were analyzed. Thermographs corresponding to gel to liquid-crystalline transition of eSM and DPPC bilayers containing Chol are shown in Fig. 2a and b, respectively. The derived parameters (T_m and ΔH) are summarized in Table 1. It is well know that

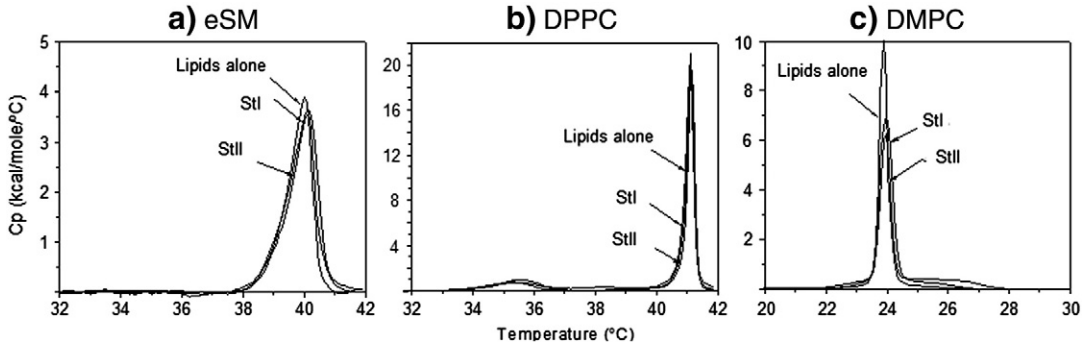

Fig. 1. DSC heating thermograms of MLV of phospholipids in the absence of cholesterol. Excess heat capacity (Cp) vs. temperature (°C) for a) eSM, b) DPPC or c) DMPC in the absence and presence of sticholysins. Lipid concentration: 1 mM. Protein:lipid molar ratio: 1:75. Samples were prepared by suspending lipids in PIPES buffer (20 mM PIPES, 140 mM NaCl, 1 mM EDTA, pH 7.4) with or without the addition of sticholysins. Scan rate: 1 °C min^{-1}.

Chol broadens and lowers the enthalpy of the gel to liquid-crystalline phase transition of phospholipids. Inclusion of low concentrations of Chol into PC and SM membranes results in a bimodal gel-to-liquid-crystalline phase transition, which can be deconvolved into two components [31,32]. As has been described [30], deconvolution resolved a lower temperature component commonly associated with the Chol-poor domain, and a higher temperature component related with the Chol-rich domain (Fig. 2a (inset) and b (inset)).

In eSM:Chol (9:1) bilayers, the characteristic transition of eSM appeared to be shifted to lower temperatures (38.5 °C) (Figs. 1a, 2a (inset) and Table 1). Moreover, the transition temperature of the higher temperature component was almost identical to that of pure eSM (Fig. 2a (upper inset) and Table 1). Additionally, the total enthalpy of the mixture decreased almost 10-fold in comparison with the Chol-free membrane (Table 1). In contrast, DSC curves in the presence of proteins were characterized by having only one transition peak around 39 °C, with no changes in the total enthalpy of the observed transition (Fig. 2a, Table 1).

With respect to the DPPC:Chol (9:1) mixture, the lower temperature transition is assigned to the Chol-poor PC domains, which appeared at 39.8 °C, and the high temperature component is assigned to the melting of the Chol-rich PC domains at 40.8 °C (Fig. 2b (inset) and Table 1). The overall main enthalpy of the mixture decreased almost 5-fold in comparison with the Chol-free membrane (Table 1). Similar to what happened with eSM:Chol (9:1), the addition of protein clearly reduced the phase separation of DPPC:Chol (9:1) membranes as evidenced by the disappearance of the two components in the endotherms, resulting in a single transition around 40 °C. No relevant changes in the total enthalpy of the process were detected in the presence of the proteins (Fig. 2b and Table 1).

Additionally, we investigated the effect of proteins on an equimolar mixture of PC and SM, also used in actinoporin studies [5]. For this, we chose DMPC, a phospholipid with the same polar head group but with shorter fatty acid chains and hence less ordered instead of DPPC, in order to assess the effect of membrane packing defects and/or phase separation on proteins interaction with lipids. Another reason to select DMPC instead of an unsaturated lipid (like DOPC) lies in the fact that phase separation is easier to detected by common DSC when using lipids with T_m higher than 0 °C, such as DMPC. Pure DMPC and pure eSM peaks were relatively sharp and cooperative as expected (Fig. 1). However, lipid mixing promoted an increase of the breadth and asymmetry of the endotherms (Fig. 2c) as well as a slight decrease in the enthalpy of the transition (Table 1). Moreover, we did not clearly resolve two transition components in the first heating scan (data not shown) but the shape of the peak indicated the existence of at least two overlapping endotherms from different lipid populations, most likely one of them enriched in DMPC and the other in eSM. The separation of components became more defined in subsequent heating and cooling scans, as previously observed by Chiu et al. [29]. Endotherms obtained in the second heating scan, upon reaching equilibrium, are shown in Fig. 2c. After deconvolution, transitions clearly appeared at 31.2 °C and 34.1 °C (Fig. 2c (inset)). Addition of protein resulted in a merging of the peaks with the formation of a more cooperative transition at ~32.6 °C. Furthermore, changes of more than 1 kcal mol^{-1} in the total enthalpy of the process were not observed except for StI (Fig. 2c and Table 1).

Table 1
Effect of sticholysins on the chain melting transition parameters of pure lipids and binary mixtures.

Lipid	Protein	T_m (°C)	ΔH (kcal mol^{-1})
eSM	–	40.1	3.9
	StI	40.0	4.5
	StII	40.1	4.0
DPPC	–	41.0	7.8
	StI	41.0	7.6
	StII	41.0	8.8
DMPC	–	23.9	4.1
	StI	24.0	4.4
	StII	24.0	4.5
eSM:Chol	–	38.5 and 40.3	0.4
(9:1)	StI	39.0	0.5
	StII	39.0	0.7
DPPC:Chol	–	39.8 and 40.8	1.4
(9:1)	StI	39.1	1.8
	StII	40.1	1.7
DMPC:eSM	–	31.2 and 34.1	3.0
(1:1)	StI	32.9	5.2
	StII	32.4	3.8

Lipid concentration was 1 mM and protein:lipid ratio 1:75. Samples were prepared by co-dissolving proteins and lipids in buffer PIPES (20 mM PIPES, 140 mM NaCl, 1 mM EDTA, pH 7.4). Scan rate: 1 °C min^{-1}. T_m is the temperature at which the chain melting transition takes place and ΔH is the total enthalpy of the transition per mol of phospholipid present. For binary mixtures, the values correspond with a heating scan obtained after reach equilibrium by a previous heating and cooling cycle. Two values of temperature correspond with different transitions obtained after the deconvolution of the thermograms.

3.3. Effect on membrane domains

In situ AFM studies of sticholysin with DOPC:eSM:Chol (1:1:1) to mimic the composition of a red blood cell membrane [33–35] were performed. This lipid mixture has frequently been used to study the co-existence of liquid-ordered (L_o) and liquid-disordered (L_d) domains [35]. This membrane composition was also selected not only in order to be more representative of biological systems but also to overcome the limitation of DSC on detecting membrane domains in highly heterogeneous systems. The DOPC:SM:Chol bilayer separated into two observable phases: the DOPC-rich L_d, and the SM/Chol-rich L_o. Before protein

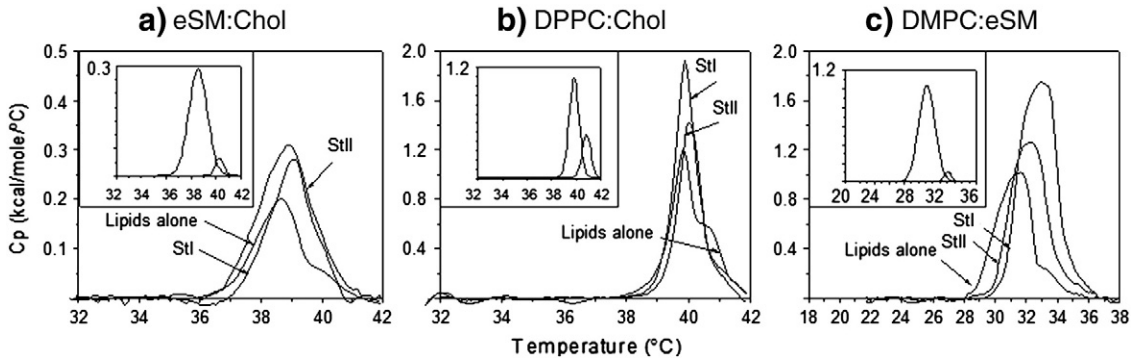

Fig. 2. DSC heating thermograms of MLV of the binary mixture of PC:SM or phospholipids:Chol. Excess heat capacity (Cp) vs. temperature (°C) for a) eSM:Chol (9:1), b) DPPC:Chol (9:1) c) DMPC:eSM (1:1) in the presence or absence of sticholysins. Lipid concentration: 1 mM. Protein:lipid ratio: 1:75. Samples were prepared by suspending lipids in PIPES buffer (20 mM PIPES, 140 mM NaCl, 1 mM EDTA, pH 7.4) with or without the addition of sticholysins. Scan Rate: 1 °C min^{-1}. Second heating scans obtained after a heating and cooling cycle are shown. Inset: deconvolution of the thermograms corresponding to the lipids alone.

addition, the SM-Chol enriched domains were ~0.8 to 1.0 nm higher than the surrounding DOPC-enriched phase (Fig. 3a, upper and lower), which corresponds well with previous results [36–38].

After binding to the bilayer, both proteins appeared to further integrate into the model membrane over time. Regions within the areas of protein addition simultaneously lowered and became smoother. Proteins that initially extended multiple nanometers above the liquid-disordered phase produced a surface that was less than a nanometer taller than the original membrane. However, we could not distinguish individual molecules inserted into the membrane but the appearance of "small blobs" in the first image after toxin addition could be representative of the initial binding events. Regardless, it is clear that upon protein addition, both StI and StII clearly modified the membrane structure. The effect started as a change in texture of the L_d domain, and L_o domains decreased in size (Fig. 3b, upper). Different regions within the membrane became smoother over time producing a surface with less than a nanometer height mismatch between domains. Additionally, we detected a loss of regular shape of the domain borders (upper Fig. 3c and d; lower Fig. 3d). The influence of StI and StII on the membrane shows that the steady-state effect was quite similar for both proteins.

4. Discussion

Both binding and pore-formation steps by actinoporins are critically dependent on the physicochemical nature of the membrane [26,39]. Thus, this investigation was aimed at gaining insight into the influence of sticholysins on membrane lipid rearrangement. For actinoporins, it has been widely accepted that binding to membranes is favored both by the presence of SM and the occurrence of membrane surface defects due to non-ideal lipid packing [19,23–25]. To test this hypothesis, we employed DSC and AFM as complementary techniques that allow for the evaluation of different membranes containing domain systems.

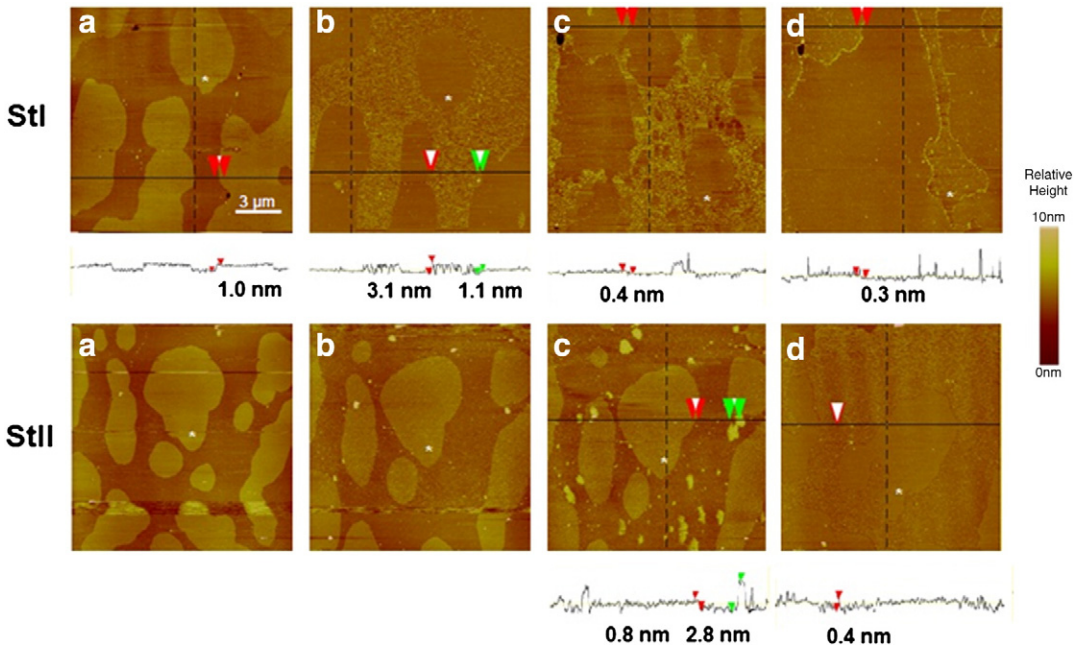

Fig. 3. Representative AFM images resulting from the remodeling of DOPC:eSM:Chol (1:1:1) membranes by sticholysins. Protein concentration: 0.25 µM. Lipid composition: DOPC:SM:Chol (1:1:1). Upper row: StI. Elapsed time: (a) before addition, and (b) 10 min, (c) 2.5 h, and (d) 3.5 h after addition. Lower row: StII. Elapsed time: (a) before addition, and (b) 0.5 h, (c) 1 h, and (d) 1.5 h after addition. The white asterisk indicates a fiduciary point. The incubation period for both proteins was the same although only representative sampling points along a continuous imaging experiment are shown. The arrows indicate the position of the height data analysis points shown in the section analysis below the figures.

The results herein presented clearly show that sticholysin's effect on the phase transition of membranes is greater for the binary DMPC:SM mixture, in contrast with the single component systems where there is essentially no effect on the phase transition (Table 1). The increase in the T_m in binary system in contrast to pure lipids is consistent with previous results obtained by DSC with the related protein EqtII [40]. However, the absence of binding to pure eSM contrasts with the assumption that SM alone is enough for protein binding [41,42] and oligomerization [42]. The discrepancy between our observations and those previously obtained by assessing protein binding to SM by Western blot, ELISA, or NMR, is possibly due to the different experimental approaches. We cannot rule out that data obtained by DSC might underestimate the binding of sticholysins to SM taking into account the low T_m shift observed even in binary systems. In spite of this contradiction, it is clear the effect of sticholysin binding on membrane domains is reflected in the shape of the thermographs wherein the phase transition peaks appear to fuse into a single one in the presence of the proteins (Fig. 2c and Table 1). This was attributed to a lipid mixing effect promoted by both proteins.

It has also been observed that Chol in the presence or the absence of SM increases actinoporin's membrane binding and permeabilizing activity [19,20,23,43]. In this study, Chol addition also resulted in StI and StII causing larger effects in the phase transition of DPPC- or SM-containing vesicles (Figs. 1a and b, 2a and b, Table 1), as a result of both sticholysins increasing the miscibility of Chol with SM or DPPC. The vesicles containing Chol clearly phase separate but protein addition leads to a merger of phases, promoting the formation of a more structurally homogeneous membrane (Fig. 2a and b). The protein's influence on membrane structure was supported by variations in the thermograph shapes, which revealed the disappearance of two transitions. As it happens for DMPC:eSM (1:1) liposomes, the main transition in the presence of sticholysins was observed between the higher and lower temperature of the deconvoluted components corresponding to the binary mixture of lipids in the absence of sticholysins. The results obtained by DSC on binary mixtures comprising eSM:Chol (9:1), DPPC:Chol (9:1), and DMPC:eSM (1:1) stress the importance of lipid heterogeneity and phase separation for StI and II binding and revealed their effect on membrane domain mixing.

As revealed by AFM, two separate stages occurred upon the addition of StI or StII to the membrane. First, the protein binds to the membrane promoting changes in both the Lo and Ld domains. Secondly, the embedded protein promotes a reduction in line tension between Lo and Ld domains as evidenced both by a decrease in the domain mismatch and changes in domain morphology (Fig. 3). In contrast to Mancheño et al. (2006) who visualized the crystal form of StII on lipid monolayers by AFM [44], we were unable to resolve individual pores. Differences in sample preparation would explain this contradiction, mainly due to the fact that we did not obtain a crystalline structure of StII oligomer in the bilayer. It is important to recognize that we are tracking the dynamics of StII association and the formation of individual structures at concentrations far below that necessary to induce two-dimensional crystallization. In fact, this has been one of the main problems for structurally characterize α-PFTs pores with high resolution [45]. However, the lipid mixing detected by DSC was also seen by AFM. In fact, this mixing could have probably favored the protein insertion into the membrane forming the observed smooth layer (Fig. 3c and d). Such an effect has been proposed for other pore-forming molecules, including antimicrobial peptides, pore forming proteins, and detergents [46]. In fact, in a study of the pro-apoptotic protein Bax, García-Sáez et al. [46] proposed that a decrease in line tension may be a general strategy of pore-forming peptides and proteins. Therefore, our results add new lines of evidence regarding the ability of different membranolytic proteins to decrease membrane domain line tension. This may represent a common mechanism of action for these peptides, rendering insertion and stabilization of an open-pore state energetically favorable.

The role of lipid phase coexistence in the mechanism of action of actinoporins has not been well established. For example, it has been proposed that phase separation promotes pore forming activity by acting as concentrating platforms. However, the tight molecular packing and acyl chain within L_o domains may create a locally ordered environment that does not readily favor protein insertion and pore formation. In fact, proteins and peptides preferentially bind to interfaces and function as detergents, reducing line tension and leading to domain dispersion [47]. The results herein obtained are in agreement with this latter hypothesis. Both DSC and AFM data suggested that sticholysins decrease line tension between lipidic phases, which could promote the formation of more suitable disordered regions (i.e. more disorded than the so-called raft L_o domains) for N-terminus insertion and pore formation by sticholysins.

Concluding remarks

The results obtained in this investigation add support to the notion that binding to membranes by actinoporins is enhanced by the presence of membrane defects and/or the phase coexistence of lipids in the bilayer. One hypothesis, sustained over the last few years, assumes that such defects might act as binding sites for actinoporins, a strategy exploited by other membranolytic polypeptides, such as antimicrobial peptides and pore-forming toxins. Our results indicated that sticholysins decrease line tension between phases, possibly inducing an asymmetric L_o/L_d bilayer that could be a suitable platform for pore formation.

Acknowledgements

This work was possible due to a collaborative project provided by the Emerging Leaders in the Americas program from the Canadian government to UR. It was partly supported by CAPES-MES and CNPq-MES (Brazil–Cuba) collaboration projects and Iberoamerican CYTED BIOTOX Network (212RT0467). UR is a grantee from IFS (4616), Sweden. MAE and CMY acknowledge support from NSERC (RGPIN: 194435).

References

[1] M.R. Yeaman, N.Y. Yount, Mechanisms of antimicrobial peptide action and resistance, Pharmacol. Rev. 55 (2003) 27–55.
[2] M.E. Lanio, V. Morera, C. Álvarez, M. Tejuca, T. Gómez, F. Pazos, V. Besada, D. Martínez, V. Huerta, G. Padrón, M.A. Chávez, Purification and characterization of two hemolysins from *Stichodactyla helianthus*, Toxicon 39 (2001) 187–194.
[3] W.R. Kem, The biology of the nematocyst, Sea Anemone Toxins: Structure and ActionAcademic Press, New York, 1988, pp. 375–405.
[4] G. Anderluh, P. Macek, Cytolytic peptide and protein toxins from sea anemones (*Anthozoa: Actiniaria*), Toxicon 40 (2002) 111–124.
[5] M. Tejuca, M. Dalla Serra, M. Ferreras, M.E. Lanio, G. Menestrina, Mechanism of membrane permeabilization by sticholysin I, a cytolysin isolated from the venom of the sea anemone *Stichodactyla helianthus*, Biochemistry 35 (1996) 14947–14957.
[6] A. Athanasiadis, G. Anderluh, P. Macek, D. Turk, Crystal structure of the soluble form of equinatoxin II, a pore-forming toxin from the sea anemone *Actinia equina*, Structure 9 (2001) 341–346.
[7] M.G. Hinds, W. Zhang, G. Anderluh, P.E. Hansen, R.S. Norton, Solution structure of the eukaryotic pore-forming cytolysin equinatoxin II: implications for pore formation, J. Mol. Biol. 315 (2002) 1219–1229.
[8] S. García-Linares, I. Castrillo, M. Bruix, M. Menéndez, J. Alegre-Cebollada, A. Martínez-Del-Pozo, J.G. Gavilanes, Three-dimensional structure of the actinoporin sticholysin I. Influence of long distance effects on protein function, Arch. Biochem. Biophys. 532 (2013) 39–45.
[9] J.M. Mancheño, J. Martin-Benito, M. Martínez-Ripoll, J.G. Gavilanes, J.A. Hermoso, Crystal and electron microscopy structures of sticholysin II actinoporin reveal insights into the mechanism of membrane pore formation, Structure 11 (2003) 1319–1328.
[10] A.E. Mechaly, A. Bellomio, D. Gil-Cartón, K. Morante, M. Valle, J.M. González-Mañas, M.A. Guérin, Structural insights into the oligomerization and architecture of eukaryotic membrane pore-forming toxins, Structure 19 (2011) 181–191.
[11] G. Anderluh, J. Pungercar, I. Krizaj, B. Strukelj, F. Gubensek, P. Macek, N-Terminal truncation mutagenesis of equinatoxin II, a pore-forming protein from the sea anemone Actinia equina, Protein Eng. 10 (1997) 751–755.
[12] Q. Hong, I. Gutiérrez-Aguirre, A. Barlič, P. Malovrh, K. Kristan, Z. Podlesek, P. Maček, D. Turk, J.M. Gonzalez-Mañas, J.H. Lakey, G. Anderluh, Two-step membrane binding

by equinatoxin II, a pore forming toxin from the sea anemone, involves an exposed aromatic cluster and a flexible helix, J. Biol. Chem. 277 (2002) 41916–41924.
[13] P. Malovrh, G. Viero, M. Dalla Serra, Z. Podlesek, J.H. Lakey, P. Macek, G. Menestrina, G. Anderluh, A novel mechanism of pore formation: membrane penetration by the N-terminal amphipathic region of equinatoxin, J. Biol. Chem. 278 (2003) 22678–22685.
[14] K. Kristan, Z. Podlesek, V. Hojnik, I. Gutiérrez-Aguirre, G. Guncar, D. Turk, J.M. González-Mañas, J.H. Lakey, P. Macek, G. Anderluh, Pore formation by equinatoxin, a eukaryotic pore-forming toxin, requires a flexible N-terminal region and a stable β-sandwich, J. Biol. Chem. 279 (2004) 46509–46517.
[15] F. Pazos, A. Valle, D. Martínez, A. Ramírez, L. Calderón, A. Pupo, M. Tejuca, V. Morera, J. Campos, R. Fando, F. Dyszy, S. Schreier, E. Horjales, C. Álvarez, M.E. Lanio, E. Lissi, Structural and functional characterization of a recombinant sticholysin I (rSt I) from the sea anemone *Stichodactyla helianthus*, Toxicon 48 (2006) 1083–1094.
[16] E.M. Cilli, F.T. Pigossi, E. Crusca Jr., U. Ros, D. Martínez, M.E. Lanio, C. Alvarez, S. Schreier, Correlations between differences in amino-terminal sequences and different hemolytic activity of sticholysins, Toxicon 50 (2007) 1201–1204.
[17] J. Alegre-Cebollada, M. Cunietti, E. Herrero-Galán, J.G. Gavilanes, A. Martínez-del-Pozo, Calorimetric scrutiny of lipid binding by sticholysin II toxin mutants, J. Mol. Biol. 382 (2008) 920–930.
[18] A.W. Bernheimer, L.S. Avigad, Properties of a toxin from the sea anemone *Stoichactis helianthus*, including specific binding to sphingomyelin, Proc. Natl. Acad. Sci. 73 (1976) 467–471.
[19] V. de los Ríos, J.M. Mancheño, A. Martínez del Pozo, C. Alfonso, G. Rivas, M. Oñaderra, J.G. Gavilanes, Mechanism of the leakage induced on lipid model membranas by the hemolytic protein sticholysin II from the sea anemone *Stichodactyla helianthus*, FEBS Lett. 455 (1999) 27.
[20] B.B. Bonev, Y.H. Lam, G. Anderluh, A. Watts, R.S. Norton, F. Separovic, Effects of the eukaryotic pore-forming cytolysin equinatoxin II on lipid membranes and the role of sphingomyelin, Biophys. J. 84 (2003) 2382–2392.
[21] B. Bakrač, I. Gutiérrez-Aguirre, Z. Podlesek, A. Sonnen, R. Gilbert, P. Maček, J. Lakey, G. Anderluh, Molecular determinants of sphingomyelin specificity of a eukaryotic pore-forming toxin, J. Biol. Chem. 283 (2008) 18665–18677.
[22] A. Drechsler, G. Anderluh, R.S. Norton, F. Separovic, Solid-state NMR study of membrane interactions of the pore-forming cytolysin, equinatoxin II, Biochim. Biophys. Acta 1798 (2010) 244–251.
[23] A. Barlič, I. Gutiérrez-Aguirre, J.M. Caaveiro, A. Cruz, M.B. Ruiz-Argüello, J. Pérez-Gil, J.M. González-Mañas, Lipid fase cohexistence favours membrane insertion of equinatoxin-II, a pore-forming toxin from *Actinia equina*, J. Biol. Chem. 279 (2004) 34209–34216.
[24] J. Alegre-Cebollada, I. Rodríguez-Crespo, J.G. Gavilanes, A. Martínez del Pozo, Detergent-resistant membranes are platforms for actinoporin pore-forming activity on intact cells, FEBS J. 273 (2006) 863–871.
[25] P. Schön, A.J. García-Sáez, P. Malovrh, K. Bacia, G. Anderluh, P. Schwille, Equinatoxin II permeabilizing activity depends on the presence of sphingomyelin and lipid phase coexistence, Biophys. J. 95 (2008) 691–698.
[26] C. Álvarez, J.M. Mancheño, D. Martínez, M. Tejuca, F. Pazos, M.E. Lanio, Sticholysins, two pore-forming toxins produced by the Caribbean Sea anemone *Stichodactyla helianthus*: their interaction with membranes, Toxicon 3457 (2009) 1–14.
[27] A. Filippov, B. Munavirov, G. Gröbner, M. Rudakova, Lateral diffusion in equimolar mixtures of natural sphingomyelins with dioleoylphosphatidylcholine, Magn. Reson. Imaging 3 (2012) 413–421.
[28] T.P.W. McMullen, R.N. McElhaney, New aspects of the interaction of cholesterol with dipalmitoylphosphatidylcholine bilayers as revealed by high-sensitivity differential scanning calorimetry, Biochim. Biophys. Acta 1234 (1995) 90–98.
[29] M.H. Chiu, C.P. Leon Wang, P.M.M. Weers, E.J. Prenner, Apolipophorin III interaction with model membranes composed of phosphatidylcholine and sphingomyelin using differential scanning calorimetry, Biochim. Biophys. Acta 1788 (2009) 2160–2168.
[30] D.A. Mannock, R.N.A.H. Lewis, T.P.W. McMullen, R.N. McElhaney, The effect of variations in phospholipid and sterol structure on the nature of lipid–sterol interactions in lipid bilayer model membranes, Chem. Phys. Lipids 163 (2010) 403–448.
[31] T.P.W. McMullen, R.N.A.H. Lewis, R.N. McElhaney, Differential scanning calorimetric study of the effect of cholesterol on the thermotropic phase behavior of a homologous series of linear saturated phosphatidylcholines, Biochemistry 32 (1993) 516–522.
[32] T.P.W. McMullen, C. Vilcheze, R.N. McElhaney, R. Bittman, Differential scanning calorimetric study of the effect of sterol side chain length and structure on dipalmitoylphosphatidylcholine thermotropic phase behavior, Biophys. J. 69 (1995) 169–176.
[33] M. Bretscher, Membrane structure: some general principles, Science 181 (1973) 622–629.
[34] B. Engelmann, S. Streich, U.M. Schönthier, W.O. Richter, J. Duhm, Changes of membrane phospholipid composition of human erythrocytes in hyperlipidemias. I: increased phosphatidylcholine and reduced sphingomyelin in patients with elevated levels of triacylglycerol-rich lipoprotein, Biochim. Biophys. Acta 1165 (1992) 32–37.
[35] R.M. Epand, A. Thomas, R. Brasseur, R.F. Epand, Cholesterol interaction with proteins that partition into membrane domains; an overview, in: R.J. Harris (Ed.), Cholesterol Binding and Cholesterol Transport Proteins, Springer, New York, 2010, pp. 253–278.
[36] H.A. Rinia, B. de Kruijff, Imaging domains in model membranes with atomic force microscopy, FEBS Lett. 504 (2001) 194–199.
[37] J.C. Lawrence, D.E. Saslowsky, J.M. Edwardson, R.M. Henderson, Real-time analysis of the effects of cholesterol on lipid raft behavior using atomic force microscopy, Biophys. J. 84 (2003) 1827–1832.
[38] S. Chiantia, J. Ries, N. Kahya, P. Schwille, Combined AFM and two-focus SFCS study of raft-exhibiting model membranes, Chemphyschem 7 (2006) 2409–2418.
[39] L. García-Ortega, J.A. Alegre-Cebollada, S. García-Linares, M. Bruix, A. Martínez-del-Pozo, J.G. Gavilanes, The behavior of sea anemone actinoporins at the water–membrane interface, Biochim. Biophys. Acta 1808 (2011) 2275–2288.
[40] N. Poklar, J. Fritz, P. Macek, G. Vesnaver, T.V. Chalikian, Interaction of the pore-forming protein equinatoxin II with model lipid membranes: a calorimetric and spectroscopic study, Biochemistry 38 (1999) 14999–15008.
[41] I. Castrillo, N.A. Araujo, J. Alegre-Cebollada, J.G. Gavilanes, A. Martinez-del-Pozo, M. Bruix, Specific interactions of sticholysin I with model membranes: an NMR study, Proteins 78 (2010) 1959–1970.
[42] P. Sanchez-Garcia, G. Chieppa, A. Desideri, S. Cannata, E. Romano, P. Luly, S. Rufini, Sticholysin II: a pore-forming toxin as a probe to recognize sphingomyelin in artificial and cellular membranes, Toxicon 60 (2012) 724–733.
[43] D. Martínez, A. Otero, C. Álvarez, F. Pazos, M. Tejuca, M.E. Lanio, I. Gutiérrez-Aguirre, A. Barlič, I. Iloro, J.L. Arrondo, J.M. González-Mañas, E. Lissi, Effect of sphingomyelin and cholesterol in the interaction of St II with lipidic interfaces, Toxicon 49 (2007) 68–81.
[44] J.M. Mancheño, J. Martín-Benito, J.G. Gavilanes, L. Vázquez, A complementary microscopy analysis of Sticholysin II crystals on lipid films: atomic force and transmission electron characterizations, Biophys. Chem. 119 (2006) 219–223.
[45] K.C. Kristan, G. Viero, M. Dalla Serra, P. Maček, G. Anderluh, Molecular mechanism of pore formation by actinoporins, Toxicon 54 (2009) 1125–1134.
[46] A.J. Garcıa-Saez, S. Chiantia, J. Salgado, P. Schwille, Pore formation by a Bax-derived peptide: effect on the line tension of the membrane probed by AFM, Biophys. J. 93 (2007) 103–112.
[47] A. Pokorny, P.F.F. Almeida, Permeabilization of raft-containing lipid vesicles by alpha-lysin: a mechanism for cell sensitivity to cytotoxic peptides, Biochemistry 44 (2005) 9538–9544.